Axial compressive behavior of circular UHPC filled high-strength steel tube (UFHST) short columns

Author(s) & Affiliation: Jiangang Wei, Fujian University of Technology; Xia Luo, Fuzhou University; Zhichao Lai, Fuzhou University; Baochun Chen, Fuzhou University.

Abstract: There is an increasing interest in using ultra-high performance concrete (UHPC) and high-strength steel in steel-concrete composite structures. This paper makes a contribution towards this by experimentally investigating the axial compressive behavior of circular UHPC filled high-strength steel tube (UFHST) short columns. A total of nine UFHST columns were tested under axial compression. The test parameter was the steel tube diameter-to-thickness ratio (13 to 32). The steel yield stress was 961 MPa (139.35 ksi), and the compressive strength of UHPC (without steel fibers) was 142 MPa (20.59 ksi). Results from the test indicated that the strength of the UFHST columns increased with decreasing steel tube diameter-to-thickness ratios. Two limit states were observed from the tests, i.e., shear failure of the concrete infill and local buckling of the steel tube. The governing limit states depend on the steel tube diameter-to-thickness ratio. Moreover, the strength enhancement and ductility of UFHST columns were discussed by using performance indices such as concrete contribution ratio (CCR), strength index (SI) and ductility index (DI). It was demonstrated that UFHST columns with thicker tube wall had better ductility, while leading to less strength enhancement or composite action.

Keywords: UHPC filled high-strength steel tube; Diameter-to-thickness ratio; Axial compression; Short columns; Compressive performance; Composite structure.

1. Introduction

Concrete filled steel tube (CFST) optimizes the use of steel and concrete materials in the virtue of the composite action which improves the strength and ductility of concrete infill and prevents the inward local buckling of steel tube. As an efficient structural component, CFST columns have been widely used in high-rise buildings and long-span bridge as compression members [1, 2].

In recent years, with the development of concrete technology, ultra-high performance concrete (UHPC) with compressive strength higher than 150 MPa (21.75 ksi) has been prepared [3, 4]. As an inevitable tendency of upgrading CFST structures, UHPC has been filled into steel tube instead of conventional concrete [5-7]. Owing to the extremely high compressive strength of UHPC, UHPC filled steel tube (UFST) column exhibits the remarkable bearing capacity [8-10]. However, the sudden load drop after reaching the ultimate strength of UHPC infill distinctly appeared in their load-displacement curves due to the serious brittleness of UHPC [6, 9, 11]. Compared with the conventional CFST column, UFST column behaves in a lower compression ductility and the composited action [5, 11]. In order to effectively restrict the crack propagation of UHPC infill, a very smaller ratio of diameter to thickness was generally used to realize much stronger lateral confinement of ordinary strength steel [6, 9]. It should be noted that this solution with very high steel usage simultaneously brings about an adverse effect on the economic advantage of composite structures. Hence, it is inescapable to find another effective solution for enhancing the lateral confinement of steel. Xiong[9, 10] employed high strength steel and experimentally investigated the mechanical performance of square UHPC filled high strength steel tube (UFHST) columns. The interesting findings were that the brittleness of UHPC infill was improve more effectively by high strength steel than using the traditional steel. In addition, UHPC had more favorable effect on

delaying the local buckling of high strength steel. Obviously, the matching combination between high strength steel and UHPC may be an effective approach to truly upgrade CFST structures towards better performance.

Currently, few studies on the mechanical performance of UFHST structures have been done, especially for circular UFHST columns. Therefore, in the interest of addressing this gap, nine circular UFHST columns under axial load were tested in this paper and the parameter analysis of the diameter/thickness ratio was implemented.

2. Experimental Program

2.1. Test Specimens

A total of nine UFHST columns with circular section were tested under axial compression. The outer diameter of steel tubes was 140 mm (5.512 in). To abate the effect of end constraint and overall buckling on the cross-sectional strength of short columns, the ratio of column length to outer diameter was designed at 3 [12]. The diameter/thickness ratio was varied from 13 to 32 by altering the thickness of steel tube. The detailed parameters of all specimens were summarized in Table 1. The nomenclature used in this table (e.g., "UFHSTs-32-1.137-1") includes the member type (e.g., "UFHSTs" means UFHST columns), nominal D/t ratio, nominal confinement factor ξ, and duplicate specimen number.

Table 1. Detailed Parameters of Test Specimens

Specimen ID	D (mm)	L (mm)	t (mm)	D/t	f_c (MPa)	f_y (MPa)	ξ	N_u (kN)
UFHSTs-32-1.137-1	140	420	4.42	32	125	1020	1.137	4516
UFHSTs-32-1.137-2								4312
UFHSTs-22-1.904-1			6.27	22		1153	1.904	5052
UFHSTs-22-1.904-2								5386
UFHSTs-22-1.904-3								5354
UFHSTs-17-1.884-1			8.36	17		813	1.884	5531
UFHSTs-17-1.884-2								5502
UFHSTs-13-2.364-1			10.46	13		773	2.364	6339
UFHSTs-13-2.364-2								6187

Note: "D" steel outer diameter; "L" column length; "t" steel tube-thickness; "f_c" cylinder concrete compressive strength; "f_y" steel yielding strain; "$\xi=(f_yA_s)/(f_cA_c)$" confinement factor, "A_s" and "A_c" are the cross-sectional area of UHPC infill and steel tube, respectively; "N_u" test axial bearing capacity. The conversion factor from "mm" to "in" is 0.039; The conversion factor from "MPa" to "ksi" is 0.145;

2.2. Material Properties of UHPC

The reinforcement of steel fiber has less contribution to improving the compressive behavior of UHPC infill under the confinement of steel tube [9, 10], hence steel fiber was eliminated from UHPC infill in this paper for simplifying the mixing process and a lower cost of preparation. The mix proportion of UHPC infill was listed in Table 2. Coarse aggregate was excluded from the mixture for achieving the dense internal structure, the maximum size of fine aggregates was less than 0.83~1.65 mm (20~10 Mesh, 0.033~0.065 in). Cement was P.O.42.5 ordinary portland cement. Silica fume, the smallest particle in the UHPC components, had a particle size of 0.1 um (0.394×10^{-4} in). Polycarboxylic superplasticizer with water-reducing rate of 25%~30% was used for

obtaining suitable workability and adequate viscosity. The flowability of UHPC measured by cement mortar fluidity tester was 234 mm (9.213 in).

Table 2. The Mix Proportions of UHPC Infill

W/B	Cementitious materials (Kg/m^3)		Quart sand (Kg/m^3)					Superplasticizer (Kg/m^3)
	Cement	Silica fume	200-100 Mesh	140 -70 Mesh	70-40 Mesh	40-20 Mesh	20-10 Mesh	
0.16	859.54	257.86	74.06	171.72	170.69	260.71	328.48	21.49

Note: W/B is ratio of water to cementitious materials in weight. The conversion factor from "Kg/m^3" to "Lb/ in^3" is 3.613×10^{-5}.

The compressive tests on cubes (100 mm, 3.937 in), prisms (100 × 100 × 300 mm, 3.937 × 3.937 × 11.811 in) and cylinders (Φ100 × 200 mm, Φ3.937 × 7.874 in) were conducted in accordance with GB/T 31387-2015[13] and ASTM C39 [14], respectively. Without the reinforcement of steel fiber, the plain UHPC was in the form of a sudden explosive failure. The cube compressive strength f_{cu} was 146 MPa (21.176 ksi), the prism compressive strength f_{ck} was 142 MPa (20.595 ksi), and the cylinder compressive strength f_c was 125 MPa (18.130 ksi). The stress-strain of cylinders was characterized by an essentially linear elastic behavior until very shortly before reaching its compressive strength. Its elastic modulus E_c was 46.1GPa (6686.238 ksi), and the peak strain ε_{cu} was 0.0031.

2.3. Material Properties of Steel

All steel tubes manufactured by hot-rolling process were the seamless tubes. The tensile properties of steel with different tube-thickness were measured by the tensile coupon tests in accordance with GB/T228.1-2010 [15], as seen in Table 3. Compared with traditional steel, high strength steel with a lower ratio of f_u/f_y (1.5 for Q345) and $\varepsilon_u/\varepsilon_y$ (50~80 for Q345), has an insignificant hardening behavior and ductility. Nevertheless, there is an increase in its elastic behavior and yield strain.

Table 3. Tensile Properties of Steel

Tube-thickness (mm)	E_s (GPa)	f_y (MPa)	f_u (MPa)	ε_y	ε_u	ε_f	f_u/f_y	$\varepsilon_u/\varepsilon_y$
4.42	202.0	1020.0	1071.0	0.0050	0.0551	0.0777	1.05	10.9
6.27	193.0	1153.0	1217.0	0.0060	0.0514	0.0742	1.06	8.6
8.36	200.0	813.0	997.0	0.0041	0.0600	0.0915	1.23	14.8
10.46	198.0	773.0	949.0	0.0039	0.0636	0.0929	1.23	16.3

Note: "E_s" steel elastic modulus; "f_y" steel tensile yielding strength; "f_u" steel tensile ultimate strength; "ε_y" steel yielding strain; "ε_u" steel ultimate strain; "ε_u" steel fracture strain. The conversion factors from "MPa" or "GPa" to "ksi" are "0.145" and "145", respectively;

Moreover, hollow steel tubes with different tube-thickness were subjected to axial load by displacement control at a rate of 0.05 mm/min (1.969×10^{-3} in/min) for investigating the compressive performance of high-strength steel. The length/diameter ratios were 2.21~2.43. The axial shortening deformations were measured by two Linear Varying Displacement Transducers (LVDTs) to capture the full axial force-strain curve. The axial strain was obtained by dividing the measured axial displacement with tube length. All hollow steel tubes failed by the propagation of local buckling, their failure modes were shown in Figure 1. The prominent outward buckling appeared on the surface of each hollow steel tube. Owing to the lateral restraint provided by the friction on the contact surface, the local buckling at the end was more pronounced than that at

other heights. The axial force-strain curve of hollow steel tubes was represented in Figure 2. It showed that there is a slight difference in compressive respond with the increase of tube-thickness. The post-peak load kept decreasing due to the propagation of local buckling. Differently, the thicker tube developed greater strain hardening until the peak strength was reached, the rate of load loss after the peak strength slowed down. These observations demonstrated that the remarkable local buckling occurred in high steel tube, and the larger tube-thickness should be used for a reliable compressive behavior with increasing steel strength.

t =4.42 t =6.27 t=8.36 t =10.46

Figure 1. Failure Modes of Tubes

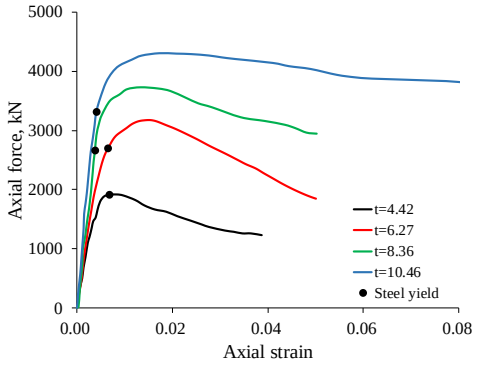

Figure 2. Axial Force-Strain of Tubes

2.4. Test Setup and Instrumentation

All test columns were placed into the testing machine with a capacity of 10000kN, and the axial load was applied directly, as shown in Figure 3. To monitor longitudinal and hoop strain of steel tube, sixteen single-strain gauges were attached to the external surface at the mid-height of steel tubes and placed at 45℃ spacing around their perimeter. The axial shortening displacements between two loading plates were measured by two Linear Varying Displacement Transducers (LVDTs) which were arranged at 180℃ apart. Four LVDTs at the mid-height of test columns and placed at 90℃ spacing around column perimeter were used to monitor the radial expansion. Axial load was applied on test column at a rate of 0.05 mm/min (1.969×10^{-3} in/min) up to the ultimate load, and this process was found to be continued well beyond the attainment of ultimate load. Achieving the shortening displacement of about 10~15 mm (0.394~0.591 in), the post-peak behavior was distinctly observed. After that, the loading rate was increased up to 1~2 mm/min (0.039~0.079 in/min) for reducing the loading time. Loading was generally terminated when the nominal axial average strain of the specimen ($\varepsilon=\Delta / L$, Δ is the axial deformation of the specimen) reached 0.06~0.008.

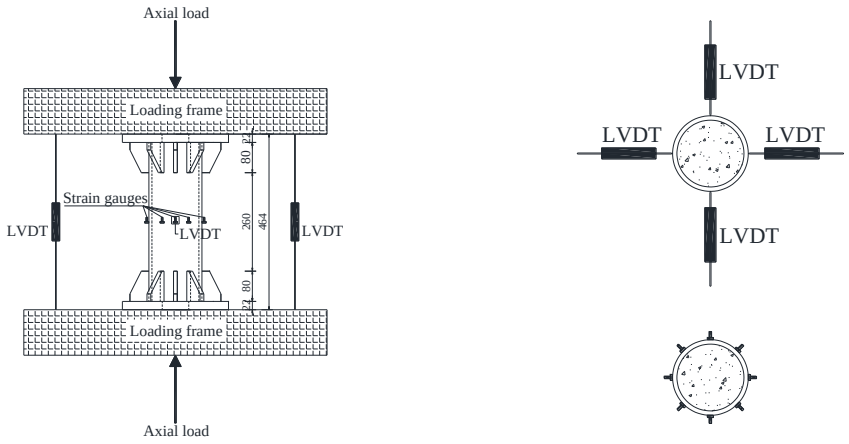

(a) Test Setup (b) Layout of LVDTS and Strain Gauges

Figure 3. Test Setup and Instrumentation

3. Results and Discussions

3.1. Failure Modes

Figure 4 represents the typical failure modes of UHFST columns. All UHFST columns with the remarkable bulges at the opposite side and an oblique slip line failed in shear failure. The external steel tubes were removed, it found that UHPC infills with a visible shear plane basically failed in the form of two intact cones. With decreasing the diameter/thickness ratio, the bulges which were followed by the slip movement between the two cones of UHSC infill along shear plane were effectively relieved, and the greater cross-sectional expansion tended to be developed. This is because the confinement of steel tube on shear failure UHPC infill become strong when the thicker tube is used.

(a) UFHSTs-32-1.137-1 (b) UFHSTs-22-1.904-1 (c) UFHSTs-17-1.884-1 (d) UFHSTs-13-2.364-1

Figure 4. Failure Modes of UHFST Columns

3.2. Structural Responds

The mean values of radial dilation (positive value) and shortening displacement (negative value) were used. Figure 5 shows the structural responds of UHFST columns under axial load. In the beginning, all curves appeared approximately linearly, the columns behaved in elastic behavior. Then, the rate of growth in radial and axial deformation started to slightly increase, indicating the occurrence of elastoplastic behavior. After reaching the peak load, a rapid increase in radial and axial deformation appeared due to the complete plastic behavior of columns. The greater diameter/thickness ratio is, the column had a larger load loss after the peak load (see UFHSTs-32-1.137). According to the failure modes of UHFST columns, the load loss was caused by the shear failure of UHPC infill. The thicker tube provided stronger confinement on restricting the shear slip

of UHPC infill, therefore less post-peak load loss occurred in columns with a smaller diameter/thickness ratio. It is interesting to note that the sudden load drop after the peak load was distinctly improved when the diameter/thickness ratio was less than 22, showing a lower steel usage for improving the brittleness of UHPC compared with the traditional steel. The hardening behavior never occurred in complete plastic stage even though the confinement factor of UFHST column achieved 2.364 (see UFHST-13-2.364), which attributes to the combined action of the striking local buckling and a lower f_u/f_y ratio of high strength steel. After the load loss, the curves tended to be horizontal, all columns possessed the residual load capacity and exhibited preeminent compressive ductility in virtue of composite action, like traditional CFST columns.

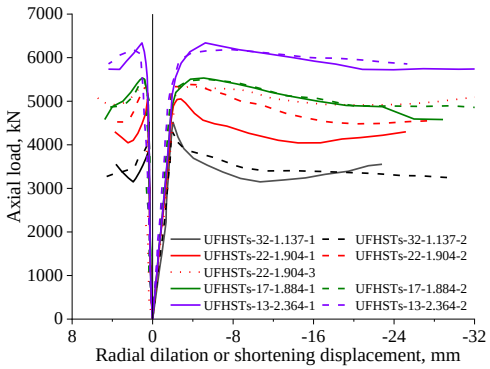

Figure 5. Structural Responds of UHFST Column under Axial Load

3.3. Composite Action

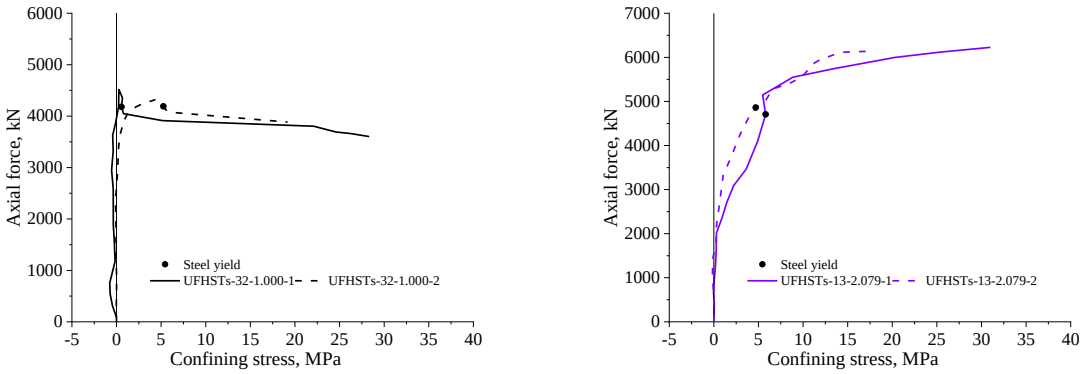

(a) D/t=32 (b) D/t=13

Figure 6. The Axial Force-Confining Stress of UFHST Columns

Steel tube and concrete infill are loaded simultaneously for CFST columns. When the composite effect is activated, the concrete infill is in the triaxial compression stress state, while the inner wall element of the steel tube is also in the triaxial stress state of longitudinal compression, radial compression and circumferential tension. To further understand the interaction between high strength steel tube and UHPC infill, the confining stresses acted on UHPC infill were obtained from the strains of steel tubes according to the relevant theory [16-19].

Figure 6 shows the typical loading history responds in confining stress of UFHST columns, where the criterion of steel yielding is that the equivalent stress is larger than f_y [16, 17]. In the

beginning, the confining stress was close to zero, indicating no interaction between steel tube and UHPC infill. Then, the confining stress started to be greater than zero, showing that the composite effect was gradually developed. Unlike UFST columns [10, 20], these observations generally appear before steel yielding, resulting in a favorable mechanical mechanism to exert the composite action [20-22]. After steel yielding, the confining stress on UHPC infill evidently increased, demonstrating that the composite effect was completely activated. The greater diameter/thickness ratio was, and the more visible load loss was observed before completely activating composite effect (see Figure 6(a)). This because larger lateral expansion (greater cracking propagation) of UHPC infill is needed to activate the same confining stress from steel tube for UHFSTs with the thinner tube-thickness.

3.4. Performance Indices

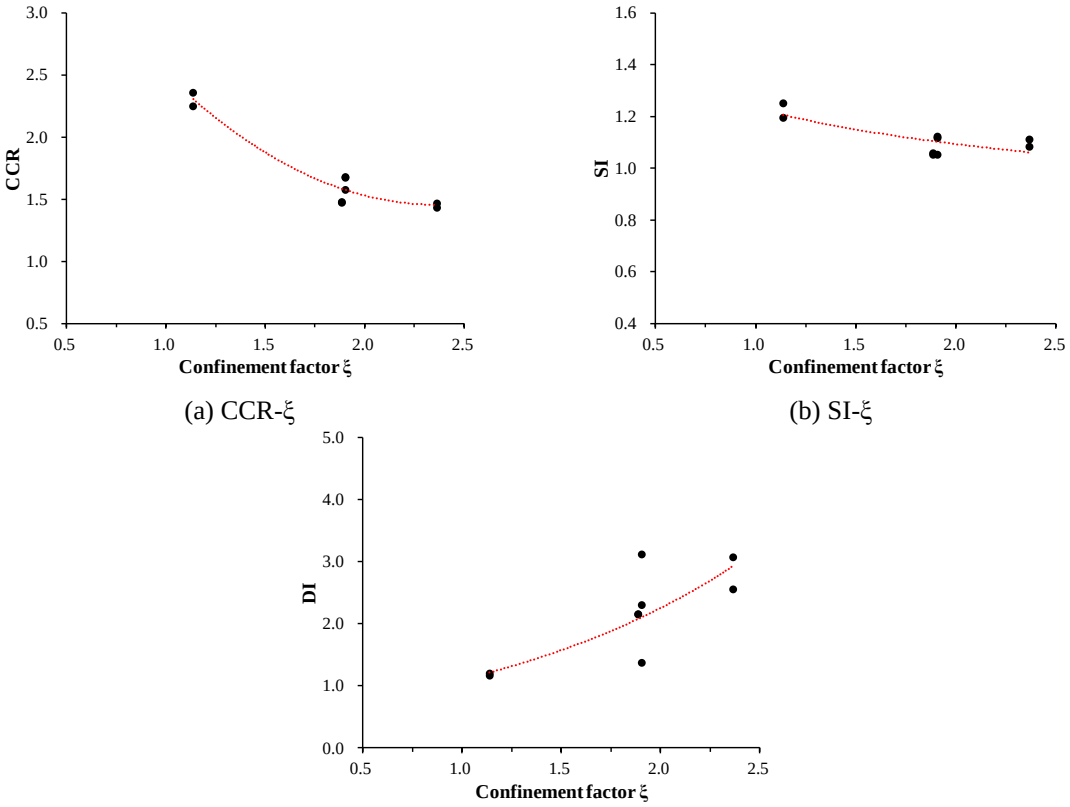

(a) CCR-ξ (b) SI-ξ

(c) DI-ξ

Figure 7. Effect of Confinement Factor on CCR, SI and DI

To evaluate the ductility and strength enhancement of UFHST columns, the relevant performance indices were defined in Equations (1)~(4).

$$\xi = \frac{f_y A_s}{f_c A_c} \tag{1}$$

$$CCR = \frac{N_{u,\,filled}}{N_{u,hollow}} \tag{2}$$

$$SI = \frac{N_{u,\,filled}}{N_{u,hollow} + A_c f_c} \tag{3}$$

$$DI = \frac{\delta_{95\%}}{\delta_u} \tag{4}$$

Here, The confinement factor ξ is the nominal strength ratio of steel tube to concrete infill; A_s and A_c are the cross-sectional areas of steel tube and concrete infill, respectively; f_y and f_c are the steel yielding stress and the cylinder concrete compressive strength, respectively; $N_{u,filled}$ represents the axial bearing capacity of UFHST columns; $N_{u,hollow}$ denotes the axial bearing capacity of hollow steel tubes measured in the test; δ_u is the axial shortening at $N_{u,filled}$; $\delta_{95\%}$ is the axial shortening when the load falls to 95% $N_{u,filled}$ (95% $N_{u,filled}$ is used instead of 85% $N_{u,filled}$, because the load drop after the peak load is less than 15% for some specimens in this paper, such as UHFSTs-13-2.079).

The strength enhancement arising from the UHPC infill is represented by concrete contribution ratio (CCR). The composite effect and the ductility performance can be evaluated by strength index (SI) and ductility index (DI), respectively. Figure 7 shows the relationships between CCR, SI or DI and confinement factor ξ. As seen in Figure 7 (a), the CCR performance index decreased with increasing confinement factor, the relative increase in CCR was 58.6% when confinement factor was reduced from 2.364 to 1.137. It indicates that much more benefits of filling UHPC into hollow steel tube for UHFST columns with thinner steel tubes than for thicker ones. This is due to more notable local buckling in thinner hollow columns. As seen in Figure 7 (b), the SI ranged from 1.05 to 1.25, indicating that the high strength steel and UHPC work well together in improving the bearing capacity of UFHST columns. Similarly, the SI decreased as the increase in the confinement factor. The relative enhancement in the SI, when confinement factor was decreased from 2.364 to 1.137 thickness, was 11.5%. It demonstrates that UHFST column with smaller confinement factor has the more significant composite effect. This is because the strength enhancement of steel tube caused by the improvement of UHPC infill on local buckling is greater than the strength enhancement of UHPC infill caused by the lateral confinement of steel tube, proving that the local bucking has a significant influence on compressive strength of high strength steel. However, as seen in Figure 7 (c), the DI tended to increase when the confinement factor was increased. The relative enhancement in the DI, increasing confinement factor from 1.137 to 2.364, was 138%. It indicates that UFHST column exhibits more ductile behavior peculiarly after the peak load when the confinement factor is increased.

4. Conclusions

This paper investigated the compressive behavior of nine UFHST columns. The following conclusions can be made from this research:

1) Notable bulges and shear plane appeared on the surface of each UFHST column. Increasing the tube thickness significantly restricts the shear slip of UHPC infill and leads to more efficient confinement.
2) With decreasing the diameter-to-thickness ratio, sudden load drop after peak load was evidently prevented. There is a smaller steel usage to improve the brittleness of UHPC infill for UFHST columns compared with UFST columns. As a result of remarkable local buckling and lower f_y/f_u ratio of high strength steel, UFHST column has no visible hardening behavior even though a strong confinement factor is used.
3) Generally, UFHST column develops composite action before steel yielding and activates it completely after steel yielding. UHPC infill confined by the thinner steel tube has a larger load loss for activating the same confining stress.

4) Filling UHPC into hollow high strength steel tube has a significant contribution on the axial bearing capacity of UFHST columns. High strength steel tube and UHPC infill can work well together. With increasing confinement factor, CCR and SI decrease. However, UFHST column exhibits more ductile behavior peculiarly after the peak load when the confinement factor is increased.

5. References

[1] Han L. H, Li W, Bjorhovde R., "Developments and advanced applications of concrete-filled steel tubular (CFST) structures: Members," *Journal of Constructional Steel Research*, Vol. 100, 2014, pp. 211-228.

[2] Chen B. C, Su J. Z, Lin S. S., "Development and application of concrete arch bridges in China," *Journal of Asian Concrete Federation*, Vol. 3, No. 1, June 2017, pp. 12-19.

[3] Chen B C, Ji T, Huang Q W et al., "Review of research on ultra-high strength concrete," *Journal of Architectural and Civil Engineering*, Vol. 31, No. 3, 2014, pp. 1-24.

[4] Fehling E., Schmidt M., Walraven J., "Ultra-High Performance Concrete UHPC: Fundamentals, Design, Examples," *Ernst & Sohn GmbH & Co. KG*, First Edition, 2014.

[5] Tue N. V., Küchler M., Schenck G. and Jürgen R., "Application of UHPC filled tubes in buildings and bridges," *Proceeding of 1st International Symposium on Ultra High Performance Concrete*, Kassel, Germany, March 2004, pp. 807-817.

[6] Guler S., Aydogan M. and Çopur A., "Axial capacity and ductility of circular UHPC-filled steel tube columns, " *Magazine of Concrete Research*, Vol. 65, No. 15, 2013, pp. 898-905.

[7] Pierre Y. Blais, Marco C., "Precast, Prestressed Pedestrian Bridge - World's First Reactive Powder Concrete Structure," *Precast/Prestressed Concrete Institute Journal*, Vol. 44, No. 5, 1999, pp. 60-71.

[8] Abbas S., Nehdi M. L., and Saleem M. A., "Ultra-High Performance Concrete: Mechanical Performance, Durability, Sustainability and Implementation Challenge," *International Journal of Concrete Structures and Materials*, Vol. 10, No. 3, September 2016, pp. 271-295.

[9] Xiong M. X., Xiong D. X., Liew, J.Y.R., "Axial performance of short concrete filled steel tubes with high- and ultra-high- strength materials," *Engineering Structures*, Vol. 136, 2017, pp. 494-510.

[10] Xiong D. X., "Structural behaviour of concrete filled steel tubes with high strength materials," *National University of Singapore*, 2012.

[11] Chen S. M., Zhang R., Jia L. J. et al, "Structural behavior of UHPC filled steel tube columns under axial loading," Thin-Walled Structures, Vol. 130, 2018, pp. 550-563.

[12] Sakino K., Nakahara H., Morino S. et al, "Behavior of centrally loaded concrete-filled steel-tube short columns," *Journal of structural engineering*, Vol. 130, No. 2, 2004, pp. 812-822. 130 (2) (2004) 180–188.

[13] National standard of People's Republic of China. Reactive powder concrete, GB/T 31387-2015, China Standard Press, 2015.

[14] Annual Book of ASTM Standards, ASTM C39, West Conshohocken, PA, 2012

[15] National standard of People's Republic of China. Metallic materials - Tensile testing - Part 1: Method of test at room temperature, GB/T228.1-2010, China Standard Press, 2010.

[16] Chakrabarty J., "Theory of plasticity," *Elsevier Butterworth-Heinemann*, 2006.

[17] Zhang SM, Guo LH, Ye ZL, et al. "Behavior of steel tube and confined high strength concrete for concrete filled RHS tubes," *Advances in Structural Engineering*, Vol. 8 No. 2, 2005, pp.101-116.

[18] Hearn E.J., "Mechanics of Materials 1- An introduction to the mechanics of elastic and plastic deformation of solids and structural materials," *Elsevier Butterworth-Heinemann*, 1997-3rd ed, pp. 215-222.

[19] Hearn E.J., "Mechanics of Materials 2- An introduction to the mechanics of elastic and plastic deformation of solids and structural materials," *Elsevier Butterworth-Heinemann*, 1997-3rd ed, pp. 87-92.

[20] Liew, J.Y.R. and Xiong, M.X., "Design Guide For Concrete Filled Tubular Members With High Strength Materials to Eurocode 4," Research Publishing, Blk 12 Lorong Bakar Batu, 349568 Singapore, 2015

[21] Zhong S. T., "Concrete-filled Steel Tube structure," Tsinghua University Press, 2003.
Liew, J.Y.R. and Xiong, M. X., Xiong D. X., "Design of Concrete Filled Tubular Beam-columns with High Strength Steel and Concrete," Structures, Vol. 8, 2016, pp. 213-226.

[22] Liew, J.Y.R. and Xiong, M. X., Xiong D. X., "Design of Concrete Filled Tubular Beam-columns with High Strength Steel and Concrete," *Structures*, Vol. 8, 2016, pp. 213-226.

6. Acknowledgements

The research presented in this paper was financially supported by the Natural Science Foundation of China (Grant No: 51578756). The support is gratefully acknowledged.